

Magmatic processes in titanite-bearing dacites, central Andes of Chile and Bolivia

SETSUYA NAKADA

Department of Earth and Planetary Sciences, Faculty of Science 33, Kyushu University, Hakozaki, Fukuoka 812, Japan

ABSTRACT

Dacites in the central Andes contain euhedral phenocrysts of titanite. In the studied dacites, pargasite phenocrysts coexist with hornblende phenocrysts, neither of which show notable compositional zoning, implying mixing of pargasite-bearing mafic magma and hornblende-bearing rhyolitic magma just before eruption. The rhyolitic magma was highly oxidized, cool, and hydrous at shallow levels in the crust and was underlain by the hotter, less-oxidized mafic magma. Titanite crystallized from the rhyolitic magma.

Titanite phenocrysts record evidence for reduction and oxidation during crystallization according to a reaction such as titanite + Ti-rich magnetite + quartz = ilmenite + calcic silicate + O. The change of f_{O_2} probably resulted from devolatilization of magma at the top of the chamber. Heating of titanite phenocrysts during mixing or unloading during eruption caused vesiculation of their melt inclusions, fragmenting the phenocrysts.

INTRODUCTION

Although it is a common mineral in plutonic and metamorphic rocks, titanite is rare in volcanic rocks (e.g., Deer et al., 1982). Compared with titanite in plutonic and metamorphic rocks (Paterson et al., 1989; Franz and Spear, 1985), volcanic titanite has not been described in detail. Ewart (1979) summarized occurrences of titanite phenocrysts in silicic volcanic rocks from the Andes, western United States, and Mediterranean regions. The stability of titanite in magmas has been discussed by several authors (Verhoogen, 1962; Carmichael and Nicholls, 1967; Lipman, 1971; Wones, 1989), who noted that it is stable in oxidized magmas. Because the occurrence of titanite phenocrysts is sensitive to f_{O_2} , its presence as a phenocryst allows us to place constraints on f_{O_2} in the magma chamber. However, experimental results of partial melting at high pressure and temperature (Yoder and Tilley, 1962; Helz, 1973; Hellman and Green, 1979; Green and Pearson, 1986a, 1986b, 1987) show that titanite is stable in hydrous silicic melts of high-Ti content regardless of f_{O_2} . Thus, important questions are whether or not titanite in volcanic rocks crystallized directly from silicate melts, and what conditions stabilize magmatic titanite.

Volcanic rocks from the central Andes, including the titanite-bearing dacites from the central Andes which I have studied, commonly show evidence for magma mixing (Thorpe et al., 1984; O'Callaghan and Francis, 1986); therefore, clarifying the mode of mixing is an important question regarding the stability of titanite. In this paper, I describe in detail titanite-bearing dacites from the central Andes and discuss the stability of titanite and magmatic processes in the silicic magma chambers.

GEOLOGICAL SETTING AND SAMPLING

The central volcanic zone of the Andes (Thorpe and Francis, 1979) is situated on continental crust with a thickness of 70 km or more (James, 1971). Sajama, Parinacota, and Porquesa Volcanoes stand near the border between Chile and Bolivia (Fig. 1). They are andesite-dacite stratovolcanoes rising upward to 5200–6500 m on an extensive ignimbrite plateau of 4000 m elevation. Neither Sajama nor Porquesa Volcano has been studied geologically or petrologically. Parinacota Volcano was studied by Katsui and Gonzalez (1968) and Wörner et al. (1988).

The summit of Sajama Volcano (Nevado de Sajama) is covered with a glacier. Parasitic lava domes and flows occur on its deeply glaciated slopes. The parasitic cones are arranged in a N70°E–S70°W direction and appear to become older with distance from the summit. Parinacota Volcano is one of a pair of volcanoes (Nevados de Payachata); Pomerape Volcano stands just to the north. The activity of Parinacota Volcano started in the Pleistocene and continues to the present (Wörner et al., 1988). This volcano records two stages of growth; glacial erosion and collapse of the volcano took place between the two stages. Porquesa Volcano consists of two adjacent cones of thick lava flows and domes (M. Takahashi, personal communication, 1989). The relationship between age and cone morphology in the Payachata volcanic field (Wörner et al., 1988) indicates that Sajama and Porquesa Volcanoes probably formed during a period extending from the late Miocene to the Pleistocene.

Titanite-bearing dacites were collected from lava flows and domes produced by different stages of eruption for each volcano: three samples from different parasitic cones

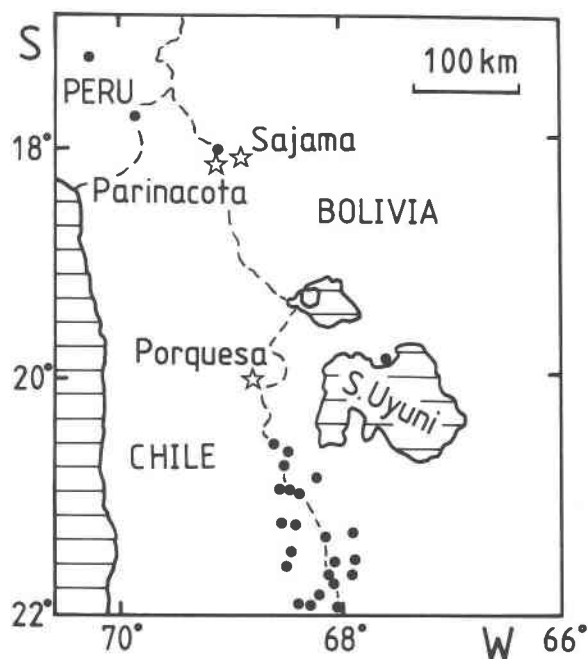


Fig. 1. Map showing distribution of Pliocene–Recent volcanic centers in the central Andes volcanic zone (dots and stars = Thorpe et al., 1982). Stars are volcanoes from which titanite-bearing dacites were sampled (Sajama Volcano, 18°07'S–68°53'W; Parinacota Volcano, 18°10'S–69°09'W; Porquesa Volcano, 19°58'S–68°44'W).

at Sajama Volcano (706, 708, and 801), two samples from the second and third stages at Parinacota Volcano (M62 and M81, respectively; Katsui and Gonzales, 1968), and two samples from different cones at Porquesa Volcano (POR-01 and POR-02). The modal compositions are listed in Table 1. All are dacites with abundant phenocrysts of plagioclase, amphibole, and biotite. Titanite phenocryst content reaches 0.4 vol%; that of quartz is characteristically low (<2%). Mg-rich olivine phenocrysts coexist with quartz and sanidine phenocrysts in the Sajama volcanic rocks. All rocks have a glassy groundmass that

contains various sizes of vesicles. The groundmass is variably devitrified, and spherulitic aggregates and crystalite pods may be present.

ANALYTICAL METHODS

Whole-rock composition was determined by X-ray fluorescence (XRF: Rigaku-GF3063P) at Kyushu University following the methods of Nakada et al. (1985) and Nakada (1987). Analytical errors for trace elements are: 50 ppm for Ba; 10 ppm for Sr, Zr, and V; 5 ppm for Rb; and 2 ppm for Nb and Y. Sr isotopic ratios of two samples from Sajama Volcano were obtained at Okayama University with the method of Kagami et al. (1982).

Chemical compositions of minerals and glass were determined at Kyushu University by a scanning electron microscope (JEOL-SEM35-CFII) equipped with an energy-dispersive spectrometer (LINK 860-2-500), using 15 kV accelerating voltage, a specimen current of 1.5 nA on iron metal, and the ZAF program (Shinno and Ishida, 1983). Glass and exsolved Fe-Ti oxide minerals were analyzed by sweeping the focused electron beam over a square area as large as possible in order to prevent sodium loss from glass and to approximate the integrated bulk composition of Fe-Ti oxide grains. Relative abundances of trace elements in titanite are considered reliable although absolute values may not be. Detection limits are 0.15, 0.35, 0.25, 0.15, and 0.15 wt% for Y_2O_3 , La_2O_3 , Ce_2O_3 , Nd_2O_3 , and Sm_2O_3 , respectively. Backscattered electron images of the titanites were observed on the same instrument. For comparison, titanites from Cretaceous granitoids in northern Kyushu (e.g., Tsusue et al., 1984) were also analyzed.

WHOLE-ROCK COMPOSITIONS

Whole-rock analyses (Table 2) show that the dacites are calcalkalic. Sr isotopic ratios of the Sajama volcanic rocks are as high as those of the Parinacota rocks (Table 2; Notsu et al., 1985). Wörner et al. (1988) have noted enrichment in large-ion-lithophile elements in the Parinacota volcanic rocks compared to other volcanic rocks in the central Andes. It is likely that volcanic rocks from this region around 18°S and far from the trench (Sajama and Parinacota) are more enriched in these elements and

TABLE 1. Modal compositions of titanite-bearing dacites

Nos.	g.m.	qz	san	plag	tit	ol	cpx	amph	bt	ap	ore
Sajama											
801	77.1	+	—	11.5	0.2	+	1.0	7.2	1.7	0.2	1.0
706	69.6	0.7	1.9	18.0	0.3	—	0.6	5.3	2.7	0.1	0.7
708	73.1	+	0.7	17.9	0.3	+	1.3	2.1	3.5	0.1	1.0
Parinacota											
M62	69.2	1.4	4.3	19.4	0.4	—	—	0.5	4.1	0.1	0.5
M81	74.3	0.1	1.5	13.7	0.3	—	0.2	7.1	1.9	0.1	0.5
Porquesa											
POR-01	71.3	0.1	0.5	22.3	0.3	—	—	4.1	0.7	+	0.5
POR-02	70.5	1.3	—	19.7	0.1	—	—	6.8	0.4	+	1.0

Note: g.m. = groundmass, qz = quartz, san = sanidine, plag = plagioclase, tit = titanite, ol = olivine, cpx = clinopyroxene, amph = amphibole, bt = biotite, ap = apatite, ore = Fe-Ti oxide minerals; + = <0.1%. All in vol%. 2000 points were counted for each sample except M62 and M81. Data for M62 and M81 are from Katsui and Gonzalez (1968). M81 contains 0.3 vol% of orthopyroxene.

TABLE 2. Chemical analyses of titanite-bearing dacites

	Sajama			Parinacota		Porquesa	
	801	706	708	M81	M62	POR-02	POR-01
SiO ₂	63.90	67.95	68.04	64.37	69.49	63.39	69.35
TiO ₂	0.92	0.72	0.68	0.96	0.57	0.93	0.62
Al ₂ O ₃	15.39	14.79	14.87	15.82	14.67	15.81	14.63
Fe ₂ O ₃ *	5.04	3.87	3.76	4.87	3.67	5.39	3.54
MnO	0.07	0.06	0.06	0.06	0.06	0.09	0.06
MgO	2.37	1.32	1.31	1.85	1.02	2.38	1.13
CaO	3.96	2.65	2.62	3.72	2.46	4.26	2.53
Na ₂ O	4.29	4.12	4.09	4.48	4.08	4.44	4.27
K ₂ O	3.79	4.29	4.35	3.50	3.82	2.99	3.67
P ₂ O ₅	0.27	0.24	0.22	0.37	0.16	0.32	0.19
Ba	1260	1230	1290	1190	1000	992	1050
Nb	9	14	13	11	10	9	8
Zr	234	233	234	215	157	169	149
Y	11	9	8	6	4	7	3
Sr	835	716	695	879	576	786	480
Rb	124	165	152	98	125	80	106
V	115	77	72	109	64	110	64
⁸⁷ Sr/ ⁸⁶ Sr	0.70665(4)	0.70664(5)	n.d.**	0.70681–0.70691†		0.70555†	0.70595†

Note: Major-element contents in wt%, recalculated on H₂O-free basis. Trace-element contents in ppm.

* Total Fe as Fe₂O₃.

** The symbol n.d. = not determined.

† Notsu et al. (1985).

Zr than rocks from elsewhere in the central volcanic zone rocks. The depletion of Y in these dacites may support the idea of Aramaki et al. (1984) and Onuma and Montoya (1984) that magmas on the continental side of the central volcanic zone evolved mainly by clinopyroxene fractionation.

PHENOCRYSTS IN DACITES

Titanite

The occurrence of titanite phenocrysts as euhedral discrete grains up to 1 mm long is a common feature of the seven samples in this study (Figs. 2 and 3). Sometimes, aggregates of titanite phenocrysts are observed (Fig. 3C). Titanite is rarely included in hornblende phenocrysts. Some titanite phenocrysts (POR-02) are surrounded by aggregates of fine, slender ilmenite crystals (Fig. 3D). Inclusions of ilmenite, hematite, rhyolite glass, and apatite are common near the core of titanite phenocrysts (Figs. 2, 3A, and 3B). In some samples, inclusions of ilmenite and hematite are concentrated along a zone in the phenocryst that represents an earlier crystal surface (M62; Fig. 2). A thin film of glass is observed around the inclusions (Figs. 2A and 2B), indicating that the Fe-Ti oxides were trapped together with melt. Titanite phenocrysts are often fragmental (Figs. 2A and 3C) and contain cracks filled with glass that appear to originate at glass inclusions (Fig. 2B). The cracks and fragmentation are likely to have resulted from expansion of the melt inclusions.

Backscattered electron images of titanite phenocrysts show zoning patterns, in which the bright zones are enriched in REE. The zoning patterns in phenocryst rims are concordant with the crystal outlines (Figs. 2C, 3B,

and 3C). However, their inner parts typically have complex zoning patterns. Phenocryst cores or inclusion areas with complex zoning patterns (Figs. 2C and 3B) recall hopper crystal forms, which are commonly found in olivine phenocrysts formed at high growth rate (Donaldson, 1976). Bacon (1989) suggested that zones enriched in accessory phases or melt inclusions within phenocrysts reflect episodes of rapid crystal growth and are distinct from zones formed by resorption of the host; rapid growth rate is thought to create a phenocryst-melt boundary layer differentiated enough for accessory-phase saturation. Although the inclusion zones of the titanite phenocrysts indeed may have formed at rapid growth rates, cores of the phenocrysts typically show corrosion textures; earlier surfaces are irregularly rounded and the concentric zonings are cut by the corrosion surfaces (Figs. 2C and 3C). Rounded and irregular forms of ilmenite inclusions surrounded by glass indicate that resorption of ilmenite took place before rapid nucleation of titanite on the ilmenite substrata. Thus, the textures of titanite phenocrysts indicate the following episodes during crystallization: (1) precipitation and later resorption of titanite; (2) ilmenite (and hematite) precipitation at titanite margins; (3) resorption of ilmenite and resumption of precipitation of titanite at rapid growth rates; (4) titanite crystal growth at relatively slow rates; and (5) fragmentation of phenocrysts.

The titanite contains small amounts of Al, Fe, and REE (Table 3, Fig. 4). Titanite in the Porquesa volcanic rocks has lower Fe, Al, and REE contents than that in the Sajama and Parinacota volcanic rocks (Fig. 4). Titanite is zoned in Ti, Ca, Al, Fe, and REE, but there are no systematic chemical changes from core to margin (Table 3).

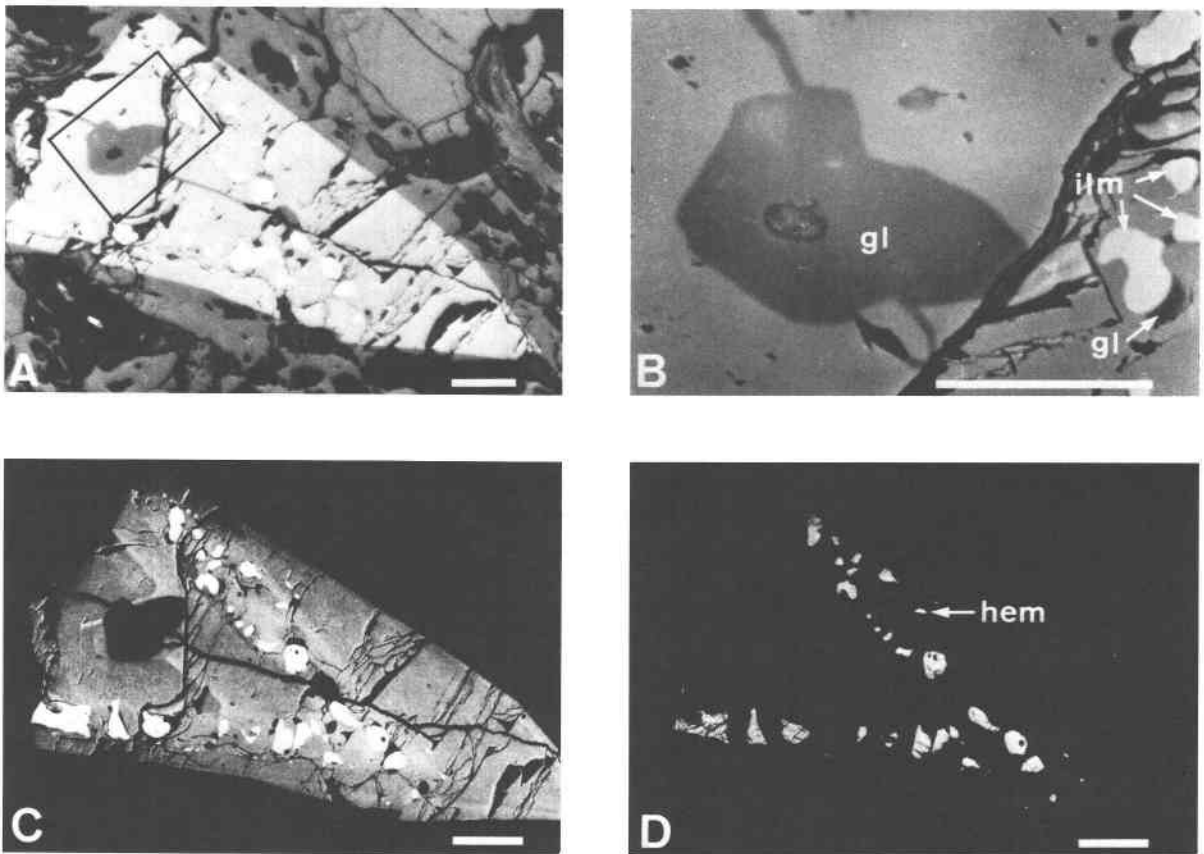


Fig. 2. Titanite phenocrysts in dacite from Parinacota Volcano (M62). Scale bar = 100 μm . (A) Photomicrograph of euhedral titanite phenocryst in reflected light. The phenocryst (light gray-colored) lost its left half prior to eruptive quenching and the broken-edge is in contact with groundmass glass. Large boxed inclusion is rhyolitic glass. (B) Photomicrograph of boxed area in A. Cracks extending from a glass inclusion (gl) are also filled with rhyolite glass. Ilmenite inclusions (ilm) are surrounded in

part by a glass film. (C) Backscattered electron image showing growth zoning. White, rounded inclusions (ilmenite and hematite) parallel the edges of the phenocryst. The growth zoning pattern is concordant with the edge of the phenocryst and with the arrangement of Fe-Ti oxide inclusions. (D) Backscattered electron image of Fe-Ti oxide inclusions. All ilmenite grains show exsolution, although hematite (hem) is homogeneous.

The zones with ilmenite and melt inclusions, or zones surrounding the resorbed cores, are usually enriched in REE (Figs. 2C and 3C). Fe content increases with Al content (Figs. 4 and 5) and with decrease in Ti content. ΣREE contents increase with decrease in Ca, and do not correlate with Ti content. A poor positive correlation exists between REE and Fe contents. Such variations were also observed in titanites from granodiorites (Paterson et al., 1989). Probably, Al (not Fe) substitutes mainly for Ti, whereas the REEs substitute for Ca.

Paterson et al. (1989) reported sector zoning of titanite from granodiorites and showed that REE contents of the fast-growing sectors are higher than those of the slow-growing sectors. This may imply that the diffusivity of Ca is lower than those of REE in silicate melts; REE were incorporated by the fast-growing titanite more easily than Ca. High REE contents in the inclusion-rich zones sur-

rounding the corroded cores of the titanite phenocrysts support rapid growth of these zones.

Amphibole

Amphibole is represented in all thin sections as euhedral large crystals of edenitic- to magnesio-hornblende, as much as 2 mm long, and as skeletal small crystals of pargasite, less than 0.5 mm long. Both amphibole samples are reddish brown in color, but some phenocrysts are opacitized. Hornblende sometimes contains Ti-rich magnetite (commonly referred to as titanomagnetite) and titanite inclusions. It occurs in aggregates with biotite, and with biotite and clinopyroxene in the Sajama volcanic rocks. Pargasite is rarely aggregated with olivine in the Sajama volcanic rocks. Amphibole grains are slightly zoned; the rims of hornblende are richer in Mg than the core, whereas the rims of pargasite are richer in Fe than

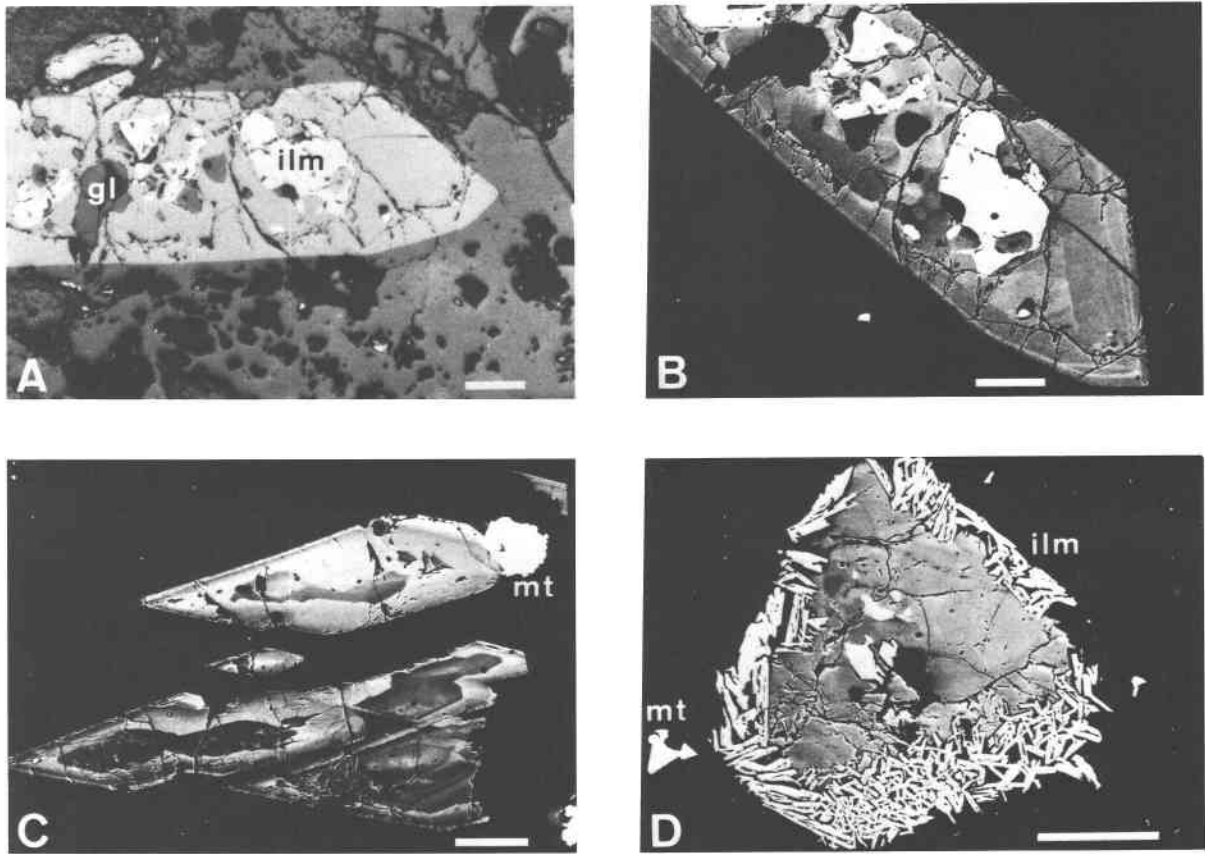


Fig. 3. Titanite phenocrysts in dacites from Porquesa and Sajama Volcanoes. Scale bar = 100 μm . (A) Photomicrograph in reflected light (POR-01). Glass (gray) and ilmenite (white) included in titanite phenocryst (light gray). (B) Backscattered electron image of A. Zoning pattern is complex in the core and simple in the rim. (C) Backscattered electron image of aggregate

of titanite phenocrysts (706); mt = Ti-rich magnetite. The grain in the lower part of the photograph is fragmented and the broken edge is in contact with groundmass glass. A titanite fragment is present in the upper right. All titanite phenocrysts have corroded cores. (D) Backscattered electron image of titanite phenocryst fringed with ilmenite needles (POR-02).

TABLE 3. Representative analyses of titanite phenocrysts

	Sajama 706		Parinacota M62			Porquesa POR-01		
	core	rim	core	mid.	rim	core	rim	
SiO ₂	29.4	28.9	29.4	29.0	29.2	29.1	30.0	
TiO ₂	36.5	35.4	36.6	37.0	36.3	37.7	37.7	
Al ₂ O ₃	1.19	1.33	1.23	1.25	1.36	1.01	0.99	
FeO*	1.45	1.82	1.50	1.41	1.48	1.20	1.31	
MnO	0.13	0.06	0.27	0.24	0.30	0.09	—	
MgO	0.09	—	—	0.11	—	—	—	
CaO	26.7	25.5	26.7	26.4	27.1	26.5	27.4	
Na ₂ O	0.06	—	—	0.27	—	—	—	
Y ₂ O ₃	—	—	—	—	—	—	0.37	
La ₂ O ₃	0.44	0.27	1.06	—	0.50	—	—	
Ce ₂ O ₃	0.43	0.74	1.07	0.67	0.86	—	0.29	
Nd ₂ O ₃	0.17	1.10	0.56	1.07	0.42	0.49	0.66	
Sm ₂ O ₃	—	—	—	0.20	0.33	—	—	
Total	96.5	95.1	98.3	97.6	97.8	96.0	98.7	
Fe/Al	0.85	0.96	0.86	0.80	0.78	0.83	0.95	

Note: Dash indicates less than the lower detection limit of the element (see text).

* Total Fe as FeO.

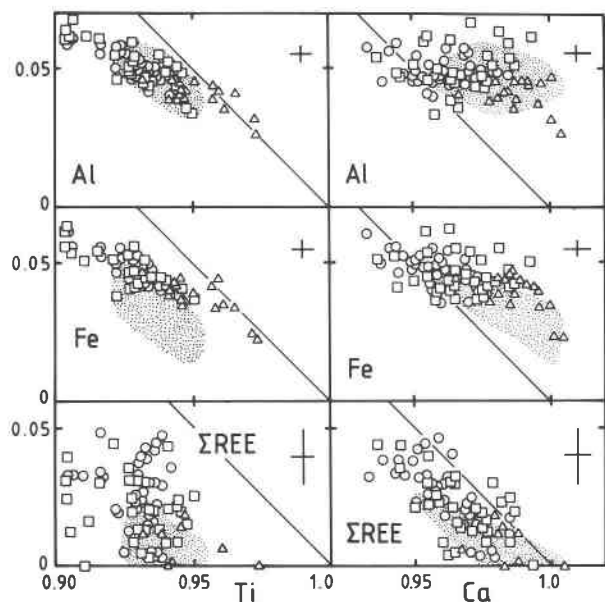


Fig. 4. Al, Fe, and Σ REE contents plotted against Ti and Ca contents for titanite phenocrysts in Andean dacites; atomic abundances calculated on a five-O atom basis. Symbols: circle, Sajama; square, Parinacota; triangle, Porquesa. Dotted area is for titanite in Japanese granitoids (Nakada, unpublished data). Crosses indicate analytical error.

the core (Table 4). However, pargasite is always more enriched in $Mg/(Mg + Fe_{tot})$, ^{41}Al , Ti, and Na than hornblende (Fig. 6). $Mg/(Mg + Fe_{tot})$ ratio ranges for pargasite are 0.75–0.68 in the Sajama volcanic rocks, 0.68–0.65 in the Parinacota volcanic rocks, and 0.74–0.62 in the Porquesa volcanic rocks. For hornblende, these ratios are 0.66–0.58, 0.64–0.62, and 0.64–0.56, respectively.

Other mafic silicates

Biotite occurs in all thin sections as flaky reddish-brown phenocrysts, less than 0.5 mm long, which do not show notable chemical zoning (Table 5). The $Mg/(Mg + Fe_{tot})$ ratio is 0.66–0.58 in the Sajama volcanic rocks, 0.60–0.58 in the Parinacota volcanic rocks (M62), and 0.54–0.53 in the Porquesa volcanic rocks (POR-02).

Olivine and pyroxene were observed only in the Sajama volcanic rocks. Euhedral olivine phenocrysts, less than 0.5 mm across, show no reaction relation with pyroxene. The olivine is normally zoned in Mg; the $Mg/(Mg + Fe_{tot})$ ratio of olivine is 0.82–0.78 (Table 6). Both diopside and Fe-rich diopside (formerly termed salite) phenocrysts are present in the dacites from Sajama Volcano. Diopside is larger (as much as 0.5 mm long) and less abundant than Fe-rich diopside; the former shows normal zoning in Mg but the latter hardly shows chemical zoning (Table 6). Wo content ranges from 42 to 44 mol% in diopside and from 45 to 47 mol% in Fe-rich diopside, whereas $Mg/(Mg + Fe_{tot})$ ratios range from 0.83 to 0.78 and from 0.77 to 0.72, respectively. The $Mg/(Mg + Fe_{tot})$ ratio of di-

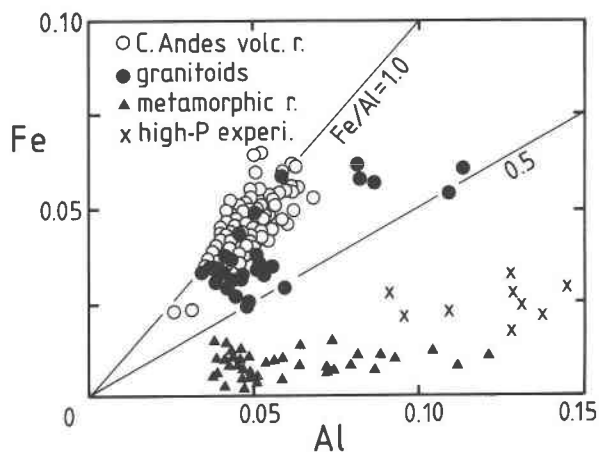


Fig. 5. Fe_{tot} plotted against Al contents for titanite phenocrysts in Andean dacites. The compositions of titanite crystals in granitoids (Gromet and Silver, 1983; Ayuso, 1984; Sawka and Chappell, 1988; Nakada, unpublished data), metamorphic rocks (Ernst and Dal Paiz, 1978; Ghent and Stout, 1984; Franz and Spear, 1985; Nishiyama, unpublished data), and products of high-temperature and high-pressure experiments (Hellman and Green, 1979; Green and Pearson, 1986b) are shown for comparison.

opside is similar to that of olivine, indicating equilibrium between olivine and diopside.

Fe-Ti oxide minerals

In all specimens, Ti-rich magnetite occurs as microphenocrysts, less than 0.5 mm across, or as inclusions in hornblende phenocrysts. It always shows exsolution textures with fine lamellae of hematite-ilmenite solid solution. Ti-rich magnetite rarely occurs in composite grains with ilmenite. Ilmenite rarely occurs as small crystals in the groundmass, which show no exsolution textures. No groundmass ilmenite could be observed in the Parinacota samples. Partitioning of Mg and Mn between Ti-rich magnetite and ilmenite grains in these dacites (Table 7) indicates equilibrium between these coexisting phases (Bacon and Hirschmann, 1988).

Other minerals

Plagioclase is the most abundant phenocryst and microphenocryst in all samples. Phenocrysts, as much as 2.5 mm long, can be either clear or dusty. The latter show the same texture as the dusty plagioclase described by Tsuchiyama (1985); a corroded crystal with a partially dissolved margin (ca. 0.1 mm thick) is mantled by a clear, thin rim (as much as 30 m thick). The chemical compositions of feldspar phenocrysts were determined only for the samples from the Sajama Volcano. In the Sajama volcanic rocks, the cores of clear microphenocrysts are the richest in Ca (An55) (Fig. 7); the most sodic compositions (An25) are found in the cores of dusty phenocrysts. The compositions of rims in both types of plagioclase approach An30. Euhedral crystals of sanidine, as much as 1.5 mm long, occur in SiO_2 -rich samples; they

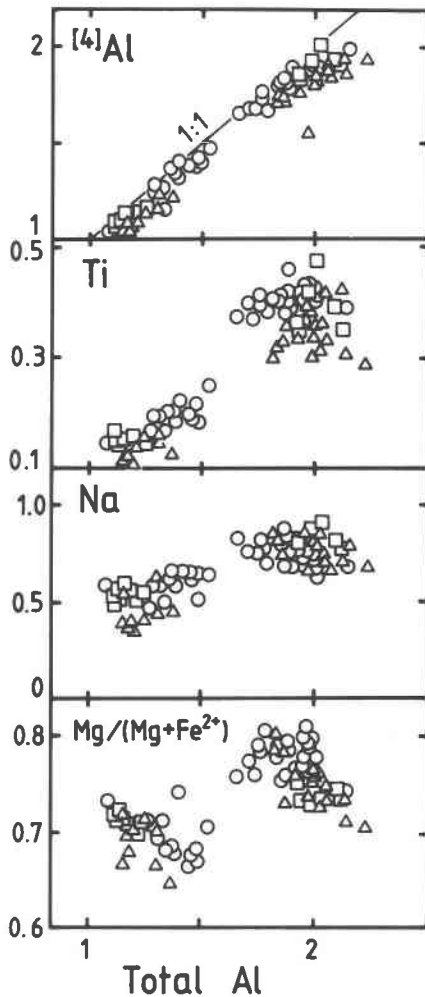


Fig. 6. Tetrahedral Al, Ti, Na, and $Mg/(Mg + Fe^{2+})$ plotted against total Al of amphibole phenocrysts in Andean dacites. Atomic abundances calculated on a 23-O atom basis. Fe^{3+}/Fe_{tot} was assumed as 0.3 according to the experimental redox conditions of Spear (1981). Symbols as in Figure 4.

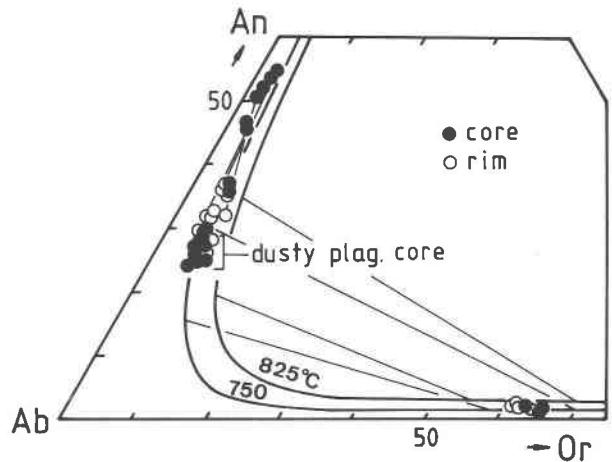


Fig. 7. Ternary An-Ab-Or plot for plagioclase and sanidine phenocrysts in dacites from Sajama Volcano. Solvi and tie lines for feldspars coexisting in equilibrium are shown for 750 °C and 825 °C at 1 kbar (Fuhrman and Lindsley, 1988).

are sometimes corroded, and zoned from Or66 to Or60 (Fig. 7). Tie lines (Fig. 7; Fuhrman and Lindsley, 1988) indicate that the sanidine is in equilibrium with the cores of dusty plagioclase. In all rocks, quartz is euhedral but corroded, and apatite is a microphenocrystic phase forming needles as much as 0.3 mm long.

Sulfide could not be identified even as inclusions of phenocrysts in this study.

INCLUSIONS IN TITANITE PHENOCRYSTS

Glass inclusions in titanite are rhyolitic and enriched in K_2O (Table 8); K_2O/Na_2O ratios are much higher than in whole-rock samples. TiO_2 contents range from 0.34 to 0.15 wt%. The normative anorthite contents are less than 4 wt%, and small amounts of normative corundum are present. High K_2O/Na_2O ratios and corundum-normative compositions may be attributed to Na migration away from the electron beam during analysis. Glass inclusions

TABLE 4. Representative analyses of coexisting amphibole phenocrysts

	Sajama (708)				Parinacota (M62)				Porquesa (POR-01)			
	Hb		Par		Hb		Par		Hb		Par	
	core	rim	core	rim	core	rim	core	rim	core	rim	core	rim
SiO ₂	46.5	48.3	42.8	42.4	47.2	47.8	41.9	41.3	47.1	46.4	41.6	43.1
TiO ₂	1.75	1.36	3.74	3.79	1.56	1.29	3.58	3.15	1.11	1.21	3.77	3.28
Al ₂ O ₃	7.47	6.35	10.3	11.0	6.87	6.20	12.3	12.2	6.75	6.88	11.8	10.9
FeO*	14.43	13.4	10.6	11.5	14.6	14.2	12.0	12.3	14.6	14.2	12.2	12.7
MnO	0.29	0.31	0.08	0.13	0.36	0.36	0.00	0.50	0.50	0.49	0.09	0.06
MgO	13.7	14.5	15.1	14.1	13.3	13.4	13.7	13.3	13.0	13.1	13.4	13.4
CaO	11.6	11.7	11.6	11.6	11.7	11.7	11.6	11.2	11.6	11.5	11.4	11.6
Na ₂ O	2.01	2.06	2.72	2.66	1.28	1.18	2.88	2.69	1.25	1.21	2.42	2.44
K ₂ O	1.09	0.79	0.94	0.97	0.76	0.71	0.89	0.87	0.67	0.76	0.54	0.65
Total	98.8	98.7	97.9	98.1	97.6	96.8	98.9	97.5	96.5	95.7	97.2	98.1
mg	62.8	65.8	71.8	68.7	61.8	62.7	67.1	65.9	61.4	62.1	66.3	65.3

Note: Par = pargasite, Hb = edenitic-hornblende to hornblende, mg = $100 \times Mg/(Mg + \Sigma Fe)$.
* Total Fe as FeO.

TABLE 5. Chemical analyses of biotite phenocrysts in titanite-bearing dacites

	Sajama					Parina	Porquesa		
	801		706	708	M62	POR-02			
	core	→ rim				core	→ rim		
SiO ₂	37.2	37.4	36.1	36.1	36.9	35.9		35.7	
TiO ₂	4.43	4.86	4.63	5.11	4.30	3.99		4.09	
Al ₂ O ₃	13.0	13.4	13.3	13.7	13.1	13.0		12.8	
FeO*	17.1	17.0	17.4	17.2	16.2	18.8		18.3	
MnO	0.15	0.02	0.24	0.14	0.09	0.28		0.24	
MgO	14.3	14.1	13.7	13.5	13.5	12.4		12.2	
Na ₂ O	1.06	0.83	0.43	0.60	1.01	0.98		0.98	
K ₂ O	9.05	9.22	9.16	9.15	8.85	9.15		9.08	
Total	96.2	96.8	94.9	95.5	93.9	94.4		93.3	
mg	59.8	59.7	58.3	58.3	59.7	53.9		54.3	

* Total Fe as FeO.

coexisting with titanite in hornblende phenocrysts are similar in composition to those in titanite (Table 8), although they are diopside normative. Postentrapment crystallization of the host crystal (titanite) on the inclusion wall causes a decrease in the TiO₂ and CaO contents of the melt inclusions, so that normative corundum contents increase in compensation for the decrease in normative anorthite content.

Ilmenite grains in titanite show subhedral to irregular, rounded forms. The ilmenite is always exsolved, such that fine lamellae of a Ti-rich phase (probably rutile) occur in the host ilmenite (Fig. 2D). The R₂O₃ content of grains of ilmenite inclusions is higher than that of groundmass ilmenite (Tables 7 and 9). Discrete, small, rounded grains of homogeneous hematite are rarely included in titanite and do not touch the ilmenite inclusions (Fig. 2D).

DISCUSSION

Composition and stability of titanite in silicate melts

The temperature- f_{O_2} relations for the reaction,
 titanite + magnetite + quartz
 = ilmenite + calcic silicate + O (1)
 were reported in Wones (1989). He concluded that higher

f_{O_2} is implied by association of the assemblage titanite + magnetite + quartz with Ca-rich pyroxene (or calcic amphibole) of higher Mg/(Mg + Fe_{tot}), and that somewhat lower f_{O_2} is implied by the same quartz-free assemblage. The absence of magnetite also reduces the f_{O_2} limit on titanite stability. The latter two conditions were employed in the experiments of Helz (1973) and Green and Pearson (1986a, 1986b, 1987), allowing titanite to crystallize from quartz- and magnetite-undersaturated melts at relatively low f_{O_2} . Nevertheless, relatively oxidized conditions may be more typical in natural silica-rich magmas, which usually contain quartz and Ti-rich magnetite phenocrysts.

High-pressure experiments (Yoder and Tilley, 1962; Helz, 1973; Hellman and Green, 1979) indicate that titanite crystallizes from hydrous partial melts of Ti-rich mafic rock only at temperatures near the wet solidus. This also implies instability of titanite in melts at atmospheric pressure. Experiments of Green and Pearson (1986a) showed that the TiO₂ content of melts saturated with Ti-rich accessory phases decreases with decreasing temperature, increasing pressure, and increasing SiO₂ content in the melt. Thus, Ti-rich accessory phases may become stable in cooled SiO₂-rich melts at crustal pressures, even if the melt is not enriched in TiO₂. In a magma chamber, residual melt will become saturated with H₂O on cooling

TABLE 6. Chemical analyses of olivine and clinopyroxene phenocrysts in titanite-bearing dacites from Sajama Volcano

	801 Olivine		801 Diopside			708 Fe-rich diopside		
	core	→ rim	core	→ rim		core	→ rim	
SiO ₂	38.8	38.1	51.4	51.4		52.4		52.6
TiO ₂	—	—	0.07	0.61		0.27		0.21
Al ₂ O ₃	0.27	0.04	2.99	3.33		0.84		0.62
FeO*	17.45	18.29	5.89	6.18		8.59		8.57
MnO	0.10	0.17	—	0.27		0.44		0.53
MgO	43.2	41.8	16.3	15.9		13.1		13.0
CaO	0.09	0.11	20.6	21.3		22.9		23.0
Na ₂ O	—	—	0.54	0.41		0.94		0.79
Total	99.9	98.5	97.8	99.4		99.5		99.3
mg	81.5	80.3	83.1	82.1		73.1		73.1

* Total Fe as FeO.

TABLE 7. Chemical analyses of Fe-Ti oxide minerals in titanite-bearing dacites

N	Sajama					Parina	Porquesa			
	801		706		708	M62	POR-02		POR-01	
	mt 4	ilm 3	mt 3	mt 8	ilm 6	mt 3	mt 3	ilm 3	mt 3	ilm 3
SiO ₂	0.36	0.69	0.57	0.61	0.40	0.71	2.05	0.93	0.51	0.43
TiO ₂	6.56	39.8	5.10	5.68	39.3	5.05	4.70	42.5	4.63	38.9
Al ₂ O ₃	1.42	0.13	1.35	1.32	0.06	1.01	2.16	0.26	1.01	0.12
Fe ₂ O ₃	53.5	21.1	55.6	54.8	27.1	55.4	52.3	18.7	56.6	25.3
FeO	33.9	31.3	33.7	34.0	31.6	34.4	34.0	33.5	33.5	31.8
MnO	0.28	0.37	0.51	0.49	0.65	0.65	0.85	1.07	0.52	0.90
MgO	1.94	2.68	0.94	1.45	1.98	0.67	1.58	2.54	0.73	1.47
CaO	0.06	0.11	0.05	0.11	0.03	0.12	0.58	0.17	0.32	0.09
Total	98.0	96.2	97.8	98.5	101.1	98.0	98.2	99.7	97.8	99.0
Mn/Mg	0.082	0.078	0.31	0.20	0.19	0.54	0.30	0.24	0.41	0.34
X _{usp}	0.187		0.149	0.164		0.150	0.145		0.136	
X _{ilm}		0.779			0.732			0.810		0.746
T (°C)	815		810				768		780	
Δlog f _{O₂}	2.4		2.7				2.6		2.9	

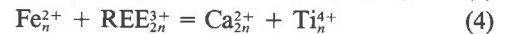
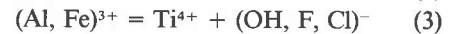
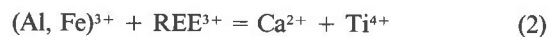
Note: mt = Ti-rich magnetite, ilm = ilmenite, N = number of area analyses. The Δlog f_{O₂} = f_{O₂} relative to FMQ. Fe₂O₃, FeO, ulvöspinel (X_{usp}), and ilmenite (X_{ilm}) contents were calculated according to Stormer (1983). The Δlog f_{O₂} and temperature were calculated according to Andersen and Lindsley (1988).

toward the wet solidus. If f_{O₂} is suitable for titanite stability, it easily crystallizes from these residual melts. Thus, titanite phenocrysts may form in low temperature silica-rich magmas that are hydrous and relatively oxidized.

The Fe/Al ratios of the Andean titanite phenocrysts are approximately 1 (Fig. 5, Table 3), as is typical for volcanic titanites (e.g., Cundari, 1979; Giannetti and Luhr, 1983; Luhr et al., 1984; Wörner and Schmincke, 1984). Fe/Al ratios in titanite from granitoids range from 0.5 to 1.0 (Fig. 5). Titanite precipitated from melts in high temperature-pressure experiments (Hellman and Green, 1979;

Green and Pearson, 1986b) has Fe/Al ratios less than 0.5. Finally, Fe/Al ratios in metamorphic titanite are much less than 0.5 (Fig. 5).

The incorporation of Al and Fe in titanite can be explained by the following substitutions (e.g., Ribbe, 1980),



Equation 2 cannot explain the chemical variations observed (Fig. 4) because Ca content has no correlation with Fe or Al contents and ΣREE content shows no correlation with Ti content. The observed variations are likely controlled by a combination of Equations 3 and 4.

Titanite from granitoids, which is typically less enriched in REE than the volcanic titanite studied, has Al contents as high as volcanic titanite, but lower Fe con-

TABLE 8. Chemical analyses of glass inclusions in titanite and hornblende phenocrysts

N	Sajama		Parinacota		Porquesa
	706 1	708 2	M62 1	M62(hb) 2	POR-01 4
SiO ₂	73.8	75.5	75.6	76.3	75.8
TiO ₂	0.32	0.34	0.15	0.31	0.22
Al ₂ O ₃	12.3	12.4	12.6	12.4	12.4
FeO*	0.84	0.35	0.59	0.75	0.61
MnO	—	0.04	0.06	0.12	0.15
MgO	0.25	0.24	0.24	0.13	0.15
CaO	0.20	0.44	0.75	0.52	0.68
Na ₂ O	3.45	3.22	2.96	3.65	2.82
K ₂ O	5.47	5.24	5.07	5.26	4.50
Total	96.6	97.7	98.0	99.4	97.3
CIPW norm					
Q	33.1	36.7	37.6	33.8	39.7
or	33.4	31.6	30.6	31.3	28.2
ab	30.2	27.8	25.6	31.1	25.3
an	1.0	1.0	3.8	1.9	3.6
C	0.3	1.1	0.8	—	1.8
di	—	—	—	0.6	—
hy	0.7	0.6	0.9	0.3	0.6
ilm	0.6	0.7	0.3	0.6	0.4
mt	0.6	0.3	0.4	0.5	0.4

Note: (hb) = glass together with titanite included in hornblende. Fe₂O₃ was assumed as 0.4 × ΣFeO_{tot} for CIPW norm.

* Total Fe as FeO.

TABLE 9. Chemical analyses of Fe-Ti oxide minerals included in titanite phenocrysts

N	Sajama		Parinacota		Porque
	706	708	M62		POR-01
	ilm 2	ilm 2	ilm 7	hm 2	ilm 6
SiO ₂	0.31	0.44	0.44	0.44	0.27
TiO ₂	33.7	33.0	34.6	11.1	37.2
Al ₂ O ₃	0.21	0.13	0.12	0.16	0.13
Fe ₂ O ₃	33.0	37.3	33.0	78.0	28.4
FeO	27.2	27.2	29.0	7.26	31.0
MnO	0.61	0.45	0.57	0.69	1.01
MgO	1.19	1.27	0.98	1.01	0.84
CaO	0.55	0.24	0.27	0.60	0.19
Total	96.8	100.0	99.0	99.3	99.0
Mn/Mg	0.30	0.21	0.32	0.38	0.69
X _{ilm}	0.660	0.629	0.669	0.195	0.716

Note: hm = hematite.

tents (Fig. 4). This fact indicates that REEs were incorporated into these titanite samples according to Equation 4 rather than Equation 2. Hellman and Green (1979) and Franz and Spear (1985) showed that Al rather than Fe^{3+} preferentially enters into the titanite structure at higher pressures. Green and Pearson (1986b) showed experimentally that substitution according to Equation 2 occurred in titanite crystallized from silicate melts at pressures greater than 7 kbar. These observations suggest that REEs are coupled with Fe^{2+} at relatively low pressure and with Al at high pressure.

Magma mixing

The coexistence of pargasite and hornblende in all dacites studied and of diopside and Fe-rich diopside in the Sajama volcanic rocks suggests mixing of two magmas. The time interval between mixing and eruption was short, as these phenocrysts do not show notable compositional zoning. This is also supported by the coexistence of Mg-rich olivine and quartz without reaction rims. The two equilibrium phenocryst assemblages before mixing can be estimated from Mg-Fe partitioning among mafic phenocrysts, phenocryst aggregation textures, and inclusion relationship: (1) hornblende + biotite + titanite + Ti-rich magnetite \pm Fe-rich diopside \pm sanidine \pm quartz + sodic, dusty plagioclase, and (2) pargasite \pm diopside \pm olivine + plagioclase. These assemblages represent rhyolitic and mafic magma, respectively. Probably, the rims of phenocrysts grew slightly in the mixed magma or were modified chemically. The outermost rims on dusty plagioclase phenocrysts may have grown in the mixed magma after rapid growth on the original crystal margin rather than after dissolution of it.

Experimental results on dissolution of plagioclase at 1 atm (Tsuchiyama, 1985) showed that the rate of partial dissolution depends on magma temperature and is extremely slow at low temperature; 100–1000 yr are necessary for a dusty zone of 100 μm width to form even at 1000 °C in a dry melt. If this is so, a more complicated scenario of magma mixing must be considered for the dacites. However, $f_{\text{H}_2\text{O}}$ may be of great importance. The morphologies of dusty plagioclase closely resemble the reaction rims on plagioclase that were obtained experimentally by Johannes (1989). His experiments on melting of plagioclase-quartz assemblages at 2-kbar H_2O pressure showed that a wide reaction rim consisting of glass and An-rich plagioclase developed around unchanged plagioclase at low temperatures during a short time; a reaction rim of approximately 50 μm width formed at 875 °C in 4 d.

T, P, and f_{O_2} conditions

Equilibration temperatures of the mafic magma at Sajama may be estimated at roughly 1000 °C, based on experimental studies of the partitioning of Fe-Mg between diopside and olivine (e.g., Grove et al., 1982). Ex-

perimental results on amphibole stability (Gilbert et al., 1982) demonstrate that the upper stability limit of pargasite in basaltic to andesitic melts is approximately 950 °C at a few kilobars and near 1050 °C at higher pressures. Coexistence of plagioclase with pargasite in a mafic magma may indicate that the magma was hydrous and at relatively low pressure, since the stability field of plagioclase is drastically reduced with increasing pressure (e.g., Green, 1982). Therefore, the equilibration temperature of the mafic magma was unlikely to have been higher than 950 °C.

A core of dusty plagioclase and sanidine in a Sajama dacite gives a temperature of approximately 750 °C with the two-feldspar geothermometer (Fuhrman and Lindsley, 1988; Fig. 7). This value is consistent with the estimated temperatures of 700–740 °C obtained from a dusty plagioclase core and hornblende with the geothermometer of Blundy and Holland (1990). Coexistence of hematite and ilmenite in the titanite phenocrysts gives information on temperature and f_{O_2} of the rhyolitic magma (Spencer and Lindsley, 1981; Burton, 1984). The f_{O_2} is approximately 1 log unit below the HM buffer, and the temperature is as low as 700 °C (Fig. 8). The rhyolitic magma is thought to have had stable hornblende, biotite, quartz, plagioclase, sanidine, titanite, and Ti-rich magnetite, all of which are required to use the geobarometer based on the Al content of hornblende (Johnson and Rutherford, 1989). The estimated pressure ranges from 1.2 to 3.3 kbar.

Magma chamber model

That all of the dacites studied show evidence of mixing between rhyolitic and mafic magmas implies that rhyolitic and mafic magmas commonly were present simultaneously beneath these volcanoes. A possible magma chamber model for the central Andean volcanoes is similar to that proposed for large-scale pyroclastic flow deposits with compositional gradients (e.g., Hildreth, 1981) or a magma chamber that is replenished by denser, more mafic magma (e.g., Huppert et al., 1982); in either case magma was stratified compositionally within the chamber, with mafic magma overlain by rhyolitic magma. In such a magma chamber, mixing between the two magmas could occur in the chamber just before eruption (e.g., Sparks et al., 1977) or in the conduit during eruption (e.g., Koyaguchi, 1985).

Temperatures deduced from the compositions of Ti-rich magnetite microphenocrysts and groundmass ilmenite in the Sajama and Porquesa volcanic rocks are 770–810 °C at an f_{O_2} of approximately 2 log units above the Ni-NiO buffer (Table 7, Fig. 8). These temperatures are higher than those estimated for the rhyolitic magma and probably lower than that of the mafic magma. Because the Fe-Ti oxide minerals are the most sensitive to physicochemical change (Bacon and Hirschmann, 1988), it is possible that the Ti-rich magnetite microphenocrysts changed composition following magma mixing. Thus,

these temperatures and f_{O_2} values may represent those of the mixed magmas.

It would be expected that heating of the rhyolitic magma during magma mixing would cause rhyolitic melt trapped in titanite phenocrysts to be oversaturated in H_2O , because H_2O solubility in silicate melts decreases with increasing temperature (e.g., Burnham and Jahns, 1962). As a result, the melt could have vesiculated and expanded during mixing and eruption so that the titanite phenocrysts were broken. Alternatively, depressurization during eruption might have been adequate to vesiculate and expand the melt inclusions.

Evidence for reduction and oxidation

Because the time interval between mixing and eruption was short in the Andean dacites, textures within the titanite phenocrysts should record physiochemical changes in the rhyolitic magma before mixing. Resorption of the titanite phenocrysts implies instability during crystallization. Titanite becomes unstable in silicate melts by the following mechanisms: (1) decreasing f_{O_2} ; (2) increasing temperature; and (3) decreasing SiO_2 or TiO_2 contents in the melt (Green and Pearson, 1986a). These conditions could have been brought about by a previous magma mixing event. However, phenocrysts coexisting with the titanite phenocrysts in these dacites show little evidence of drastic changes in the composition of coexisting melts during their crystallization before mixing.

The occurrence of resorbed crystals of titanite surrounded by ilmenite coronas in the studied dacites (Fig. 3D) implies reaction between titanite and ilmenite before or during eruption, as suggested by Czamanske (1988). Because hornblende, Ti-rich magnetite, and quartz were present in the rhyolitic magma from which titanite crystallized, a reduction reaction such as Equation 1 was probably responsible for resorption of titanite and growth of ilmenite. The ilmenite inclusion zones in titanite phenocrysts (Fig. 2) record a similar event, although ilmenite inclusions are more enriched in R_2O_3 than the corona ilmenite. Overgrowth of titanite on the ilmenite inclusion zones indicates a return to a more oxidizing condition (Eq. 1). Czamanske (personal communication, 1989) has similarly interpreted identical textures found in titanite in granodiorites of the high-level granitoids at Questa, New Mexico. Ilmenite was partly resorbed and enclosed along with melt within newly precipitated titanite. The $FeTiO_3$ component was preferentially extracted from the ilmenite inclusions once oxidation resumed, so that their bulk compositions shifted toward Fe_2O_3 , leading to precipitation of hematite as they reached the ilmenite-hematite solvus.

Mafic silicates may also reflect oxidation and reduction in the magma. Hornblende and biotite were abundant mafic silicates in the silicic magmas, and these minerals show little chemical zoning in these Andean dacites. Both minerals contain Fe^{3+} as well as Fe^{2+} , so that $Mg/(Mg + Fe_{tot})$ may not have changed measurably during the excursion in f_{O_2} that was critical to titanite stability.

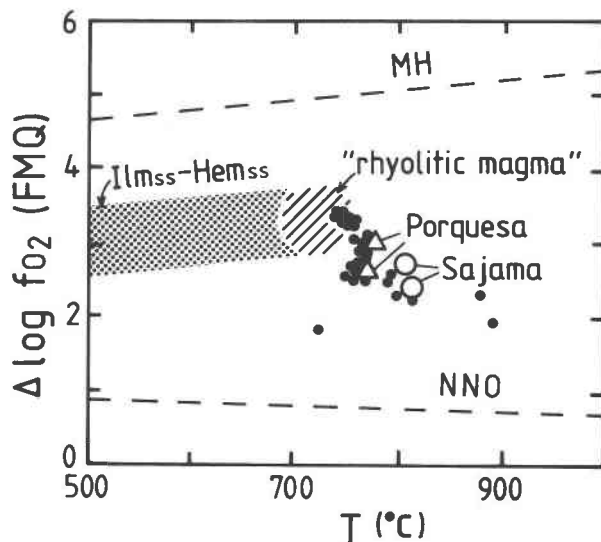


Fig. 8. Oxygen fugacity relative to FMQ ($A \log f_{O_2}$) plotted against temperature for Andean dacites. Oxygen fugacities and temperatures were estimated from Ti-rich magnetite microphe-nocrysts and groundmass ilmenite according to Andersen and Lindsley (1988) using the Stormer (1983) recalculation of analyses. Dots for titanite-bearing volcanic rocks from the literature of Lipman (1971) and Whitney and Stormer (1985), whose data were also recalculated by the above methods. The field labeled Ilm_{ss} - Hem_{ss} represents the coexisting ilmenite and hematite solid solutions (Spencer and Lindsley, 1981).

Reduction and oxidation in the magma chamber

The f_{O_2} values deduced for the mixed magmas are approximately 2 log units above the Ni-NiO buffer, and those for the rhyolitic magmas are roughly 1 log unit higher (Fig. 8), implying differences in f_{O_2} between the rhyolitic and mafic magmas. Czamanske and Wones (1973) reported increasing f_{O_2} with crystallization in the Finnmarka Intrusive Complex. The f_{O_2} -temperature relations for titanite-bearing dacites-rhyolites from the San Juan Mountains, Colorado (Lipman, 1971; Whitney and Stormer, 1985) show a similar trend; relative to buffer curves, f_{O_2} increased with cooling (Fig. 8). Calculation of chemical mass transfer based on thermodynamic relations (Ghiorso and Carmichael, 1985) showed that f_{O_2} of residual liquids undergoes a relative increase during crystallization in a system closed to O. Oxidation in the rhyolitic magma may be caused by the loss of H_2 gas during devolatilization of magma (Czamanske and Wones, 1973; Burnham, 1979; Czamanske, 1988) or by contamination with ground water and pyrite-bearing country rocks (Gerlach and Nordlie, 1975; Whitney and Stormer, 1983).

As SO_2 is the principal S gas species in highly oxidized magmas, escape of SO_2 -rich gas from magma may cause reduction of the residual magmas (Gerlach and Nordlie, 1975; Whitney, 1984; Carmichael and Ghiorso, 1986). Loss of S-rich gas from hydrous magma can suppress the

oxidizing trend due to crystallization, devolatilization, or contamination; as a result, titanite may be resorbed and an ilmenite corona may form. Because S contents in highly oxidized silicic melts are very low (e.g., Carmichael and Ghiorso, 1986), S in the magma is consumed by escape of SO₂ gas in the early stage of degassing (Gerlach and Nordlie, 1975; Burnham, 1979). The successive degassing will cause the magma to oxidize rapidly due to H₂ gas escape. The rapid growth of titanite in inclusion zones may be promoted by such oxidation.

SUMMARY

Titanite-bearing dacites from the central volcanic zone of the Andes commonly show evidence of magma mixing. Hornblende and pargasite phenocrysts coexist in all the studied dacites as a result of mixing between pargasite-bearing mafic magma and hornblende-bearing rhyolitic magma. Two populations of clear (less sodic) and dusty (more sodic) plagioclase phenocrysts are present. In some samples, unreacted olivine and quartz phenocrysts coexist. The time intervals between mixing and eruption are thought to have been short, such that reaction rims were slightly formed on the amphibole and plagioclase.

The rhyolite magmas were relatively cool, hydrous, and highly oxidized at shallow levels in the crust, whereas the mafic magmas were hotter and less oxidized. In the magma chambers, the rhyolitic magmas may have been underlain by the mafic magmas. Titanite crystallized from the rhyolitic magma. Reduction events in the magma chambers were recorded in titanite phenocrysts by Fe-Ti oxide and melt inclusion zones and irregular zoning patterns. Overgrowth of titanite on the inclusion zones records oxidation that occurred after the reduction events. The changes from reduction to oxidation may have resulted from escape of S-rich gas from the rhyolite magmas in the early stages of devolatilization and of S-deficient gas in the later stages. Finally, titanite phenocrysts were fragmented because of expansion of melt inclusions caused by heating during mixing or unloading during eruption.

ACKNOWLEDGMENTS

Valuable comments and discussions for this study by C.R. Bacon, G. K. Czamanske, T. Yanagi, and T. Nishiyama are appreciated. Critical reviews by G.K. Czamanske, C.R. Bacon, J.F. Luhr, J.A. Whitney, and P.A. Candela are greatly appreciated. I wish to thank I. Shinno and K. Ishida for providing the facility for the EDS analyses; H. Honma and Y. Okamoto for Sr isotopic analyses; E. Soria for his assistance in collecting dacite samples from Sajama; Y. Katsui for the Parinacota samples; M. Takahashi, the late N. Onuma, K. Notsu, A. Lahsen, and H. Moreno-L for the Porquesa samples and their geologic implications; and T. Nishiyama for his permission to use unpublished data on metamorphic titanites. I thank also N. Shimada and A. Sugaki for giving me a chance to stay in La Paz and JICA for financial support.

REFERENCES CITED

- Andersen, D.J., and Lindsley, D.H. (1988) Internally consistent solution models for Fe-Mg-Mn-Ti oxides: Part I. Fe-Ti oxides. *American Mineralogist*, 73, 714-726.
- Aramaki, S., Onuma, N., and Portillo, F. (1984) Petrography and major element chemistry of the volcanic rocks of the Andes, southern Peru. *Geochemical Journal*, 18, 217-232.
- Ayuso, R.A. (1984) Field relations, crystallization, and petrology of reversely zoned granitic plutons in the Bottle Lake Complex, Maine. U.S. Geological Survey Professional Paper 1320, 58 p.
- Bacon, C.R. (1989) Crystallization of accessory phases in magmas by local saturation adjacent to phenocrysts. *Geochimica et Cosmochimica Acta*, 53, 1055-1066.
- Bacon, C.R., and Hirschmann, M.M. (1988) Mg/Mn partitioning as a test for equilibrium between coexisting Fe-Ti oxides. *American Mineralogist*, 73, 57-61.
- Blundy, J.D., and Holland, J.B. (1990) Calcic amphibole equilibria and a new amphibole-plagioclase geothermometer. *Contributions to Mineralogy and Petrology*, 104, 208-224.
- Burnham, C.W. (1979) Magmas and hydrothermal fluids. In H.L. Barnes, Ed., *Geochemistry of hydrothermal ore deposits* (2nd edition), p. 71-136. Wiley, New York.
- Burnham, C.W., and Jahns, R.H. (1962) A method for determining the solubility of water in silicate melts. *American Journal of Science*, 260, 721-745.
- Burton, B.P. (1984) Thermodynamic analysis of the system Fe₂O₃-FeTiO₃. *Physics and Chemistry of Minerals*, 11, 132-139.
- Carmichael, I.S.E., and Ghiorso, M.S. (1986) Oxidation-reduction relations in basic magma: A case for homogeneous equilibria. *Earth and Planetary Science Letters*, 78, 200-210.
- Carmichael, I.S.E., and Nicholls, J. (1967) Iron-titanium oxides and oxygen fugacities in volcanic rocks. *Journal of Geophysical Research*, 72, 4665-4687.
- Cundari, A. (1979) Petrogenesis of leucite-bearing lavas in the Roman volcanic region, Italy. The Sabatini lavas. *Contributions to Mineralogy and Petrology*, 70, 9-21.
- Czamanske, G.K. (1988) Interplay between REE-bearing accessory minerals and silicic magma, Questa, New Mexico, U.S.A. Fifth international symposium on tin/tungsten granites in southeast Asia and western Pacific (Matsue). *IGCP 220 Abstracts with Program*, 25-29.
- Czamanske, G.K., and Wones, D.R. (1973) Oxidation during magmatic differentiation, Finnmarka Complex, Oslo area, Norway: Part 2, The mafic silicates. *Journal of Petrology*, 14, 349-380.
- Deer, W.A., Howie, R.A., and Zussman, J. (1982) *Sphene*. In *Rock-forming minerals*, vol 1A: Orthosilicates (2nd edition), p. 443-466. Longman, London.
- Donaldson, C.H. (1976) An experimental investigation of olivine morphology. *Contributions to Mineralogy and Petrology*, 57, 187-213.
- Ernst, W.G., and Dal Paiz, G.V. (1978) Mineral parageneses of eclogitic rocks and related mafic schists of the Piemonte ophiolite nappe, Breuil-St. Jacques area, Italian western Alps. *American Mineralogist*, 63, 621-640.
- Ewart, A. (1979) A review of the mineralogy and chemistry of Tertiary-Recent dacitic, latitic, rhyolitic and related silicic volcanic rocks. In F. Barker, Ed., *Trondhjemites, dacites, and related rocks*, p. 11-121. Elsevier, Amsterdam.
- Franz, G., and Spear, F.S. (1985) Aluminous titanite (sphene) from the eclogite zone, south-central Tauern Window, Austria. *Chemical Geology*, 50, 33-46.
- Fuhrman, M.L., and Lindsley, D.H. (1988) Ternary-feldspar modelling and thermometry. *American Mineralogist*, 73, 201-215.
- Gerlach, T.M., and Nordlie, B.E. (1975) The C-O-H-S gaseous system, part III: Magmatic gases compatible with oxides and sulfides in basaltic magmas. *American Journal of Science*, 275, 395-410.
- Ghent, E.D., and Stout, M.Z. (1984) TiO₂ activity in metamorphosed pelitic and basic rocks: Principles and applications to metamorphism in southeastern Canadian Cordillera. *Contributions to Mineralogy and Petrology*, 86, 248-255.
- Ghiorso, M.S., and Carmichael, I.S.E. (1985) Chemical mass-transfer in magmatic processes, II. Applications in equilibrium crystallization, fractionation and assimilation. *Contributions to Mineralogy and Petrology*, 90, 121-141.
- Giannetti, B., and Luhr, J.F. (1983) The White trachytic tuff of Roccamonfina Volcano (Roman Region, Italy). *Contributions to Mineralogy and Petrology*, 84, 235-252.
- Gilbert, M.C., Helz, R.T., Popp, R.K., and Spear, F.S. (1982) Experimental studies of amphibole stability. In *Mineralogical Society of America Reviews in Mineralogy*, 9B, 229-353.
- Green, T.H. (1982) Anatexis of mafic crust and high pressure crystalli-

- zation of andesite. In R.S. Thorpe, Ed., *Andesites: Orogenic andesites and related rocks*, p. 465–487, Wiley, New York.
- Green, T.H., and Pearson, N.J. (1986a) Ti-rich accessory phase saturation in hydrous mafic-felsic compositions at high P,T. *Chemical Geology*, 54, 185–201.
- (1986b) Rare-earth element partitioning between sphene and coexisting silicate liquid at high pressure and temperature. *Chemical Geology*, 55, 105–119.
- (1987) An experimental study of Nb and Ta partitioning between Ti-rich minerals and silicate liquids at high pressure and temperature. *Geochimica et Cosmochimica Acta*, 51, 55–62.
- Gromet, L.P., and Silver, L.T. (1983) Rare earth element distributions among minerals in a granodiorite and their petrogenetic implications. *Geochimica et Cosmochimica Acta*, 47, 925–939.
- Grove, T.L., Gerlach, D.C., and Sando, T.W. (1982) Origin of calc-alkaline series lavas at Medicine Lake Volcano by fractionation, assimilation and mixing. *Contributions to Mineralogy and Petrology*, 80, 160–182.
- Hellman, P.L., and Green, T.H. (1979) The role of sphene as an accessory phase in the high-pressure partial melting of hydrous mafic compositions. *Earth and Planetary Science Letters*, 42, 191–201.
- Helz, R.T. (1973) Phase relations of basalts in their melting range at $P_{H_2O} = 5$ kb as a function of oxygen fugacity. *Journal of Petrology*, 14, 249–302.
- Hildreth, W. (1981) Gradients in silicic magma chambers: Implications for lithospheric magmatism. *Journal of Geophysical Research*, 86, 10153–10192.
- Huppert, H.E., Turner, J.S., and Sparks, R.S.J. (1982) Replenished magma chambers: Effects of compositional zonation and input rates. *Earth and Planetary Science Letters*, 57, 345–357.
- James, D.E. (1971) Andean crustal and upper mantle structure. *Journal of Geophysical Research*, 76, 3246–3271.
- Johannes, W. (1989) Melting of plagioclase-quartz assemblages at 2 kbar water pressure. *Contributions to Mineralogy and Petrology*, 103, 270–276.
- Johnson, M.C., and Rutherford, M.J. (1989) Experimental calibration of the aluminum-in-hornblende geobarometer with application to Long Valley caldera (California) volcanic rocks. *Geology*, 17, 837–841.
- Kagami, H., Okano, O., Sudo, H., and Honma, H. (1982) Isotopic analysis of Rb and Sr using a full automatic thermal ionization mass spectrometer. *Papers of Institute for Thermal Spring Research (Okayama University)*, 52, 51–70 (in Japanese).
- Katsui, Y., and Gonzalez, F.O. (1968) *Geologia del area neovolcanica de los Nevados de Payachata*. Publicacion, Facultad de Ciencias Fisicas y Matematicas, Departamento de Geologia (Universidad de Chile) 29, 1–61.
- Koyaguchi, T. (1985) Magma mixing in a conduit. *Journal of Volcanology and Geothermal Research*, 25, 365–369.
- Lipman, P.W. (1971) Iron-titanium oxide phenocrysts in compositionally zoned ash-flow sheets from southern Nevada. *Journal of Geology*, 79, 438–456.
- Luhr, J.F., Carmichael, I.S.E., and Varekamp, J.C. (1984) The 1982 eruptions of El Chichon Volcano, Chiapas, Mexico: Mineralogy and petrology of the anhydrite-bearing pumice. *Journal of Volcanology and Geothermal Research*, 23, 69–108.
- Nakada, S. (1987) X-ray fluorescence determination of trace elements in silicate rocks (part 2). *Science Reports of Department of Geology (Kyushu University)*, 15, 37–44 (in Japanese).
- Nakada, S., Yanagi, T., Maeda, S., Fang, D., and Yamaguchi, M. (1985) X-ray fluorescence analysis of major elements in silicate rocks. *Science Reports of Department of Geology (Kyushu University)*, 14, 103–115 (in Japanese).
- Notsu, K., Takahashi, M., Onuma, N., Ui, T., Moreno, H.R., and Lahsen, A. (1985) Strontium isotope compositions of late Cenozoic volcanic rocks from northern Chile between latitudes 17°S and 20°S. In M. Tagiri, Ed., *Geochemical investigation of the southern Andes volcanic belt, 1982–1984*. Overseas Scientific Research (No. 59043009) p. 195–216, Ibaraki University–Universidad de Chile.
- O'Callaghan, L.J., and Francis, P.W. (1986) Volcanological and petrological evolution of San Pedro Volcano, Provincia El Loa, North Chile. *Journal of Geological Society, London*, 143, 275–286.
- Onuma, N., and Montoya, M. (1984) Sr/Ca-Ba/Ca systematics of volcanic rocks from the central Andes, southern Peru, and its implication for Andean magmatism. *Geochemical Journal*, 18, 251–262.
- Paterson, B.A., Stephens, W.E., and Herd, D.A. (1989) Zoning in granitoid accessory minerals as revealed by backscattered electron imagery. *Mineralogical Magazine*, 53, 56–61.
- Ribbe, P.H. (1980) Titanite. In *Mineralogical Society of America Reviews in Mineralogy*, 5, 137–154.
- Sawka, W.N., and Chappell, B.W. (1988) Fractionation of uranium, thorium, and rare earth elements in a vertically zoned granodiorite: Implications for heat production distributions in the Sierra Nevada batholith, California, U.S.A. *Geochimica et Cosmochimica Acta*, 52, 1131–1143.
- Shinno, I., and Ishida, K. (1983) Quantitative electron microprobe analysis of silicates and sulfides using energy-dispersive X-ray spectrometry. *Reports on Earth Science, College of General Education (Kyushu University)*, 23, 25–33 (in Japanese).
- Sparks, R.S.J., Sigurdsson, H., and Wilson, L. (1977) Magma mixing: A mechanism of triggering acid explosive eruptions. *Nature*, 267, 315–318.
- Spear, F.S. (1981) An experimental study of hornblende stability and compositional variability in amphibolite. *American Journal of Science*, 281, 697–734.
- Spencer, K.I., and Lindsley, D.H. (1981) A solution model for coexisting iron-titanium oxides. *American Mineralogist*, 66, 1189–1201.
- Stormer, J.C.J. (1983) The effects of recalculation on estimates of temperature and oxygen fugacity from analyses of multicomponent iron-titanium oxides. *American Mineralogist*, 68, 586–594.
- Thorpe, R.S., and Francis, P.W. (1979) Variations in Andean andesite compositions and their petrogenetic significance. *Tectonophysics*, 57, 53–70.
- Thorpe, R.S., Francis, P.W., Hammill, M., and Baker, M.C.W. (1982) The Andes. In R.S. Thorpe, Ed., *Andesites: Orogenic andesites and related rocks*, p. 187–205, Wiley, New York.
- Thorpe, R.S., Francis, P.W., and O'Callaghan, L.J. (1984) Relative roles of source composition, fractional crystallization and crustal contamination in the petrogenesis of Andean volcanic rocks. *Philosophical Transactions of Royal Society, London*, A310, 675–692.
- Tsuchiyama, A. (1985) Dissolution kinetics of plagioclase in the melt of the system diopside-anorthite-albite, and origin of dusty plagioclase in andesite. *Contributions to Mineralogy and Petrology*, 89, 1–16.
- Tsusue, A., Mizuta, T., and Hashimoto, K. (1984) Granitic rocks in northern Kyushu. *Mining Geology (Japan)*, 34, 385–399.
- Verhoogen, J. (1962) Distribution of titanium between silicates and oxides in igneous rocks. *American Journal of Science*, 260, 211–220.
- Whitney, J.A. (1984) Fugacities of sulfur gases in pyrrhotite-bearing silicic magmas. *American Mineralogist*, 69, 69–78.
- Whitney, J.A., and Stormer, J.C.J. (1983) Igneous sulfides in the Fish Canyon Tuff and the role of sulfur in calc-alkaline magmas. *Geology*, 11, 99–102.
- (1985) Mineralogy, petrology, and magmatic conditions from the Fish Canyon Tuff, central San Juan volcanic field, Colorado. *Journal of Petrology*, 26, 726–762.
- Wones, D.R. (1989) Significance of the assemblage titanite + magnetite + quartz in granitic rocks. *American Mineralogist*, 74, 744–749.
- Wörner, G., and Schmincke, H.U. (1984) Mineralogy and chemical zonation of the Laacher See tephra sequence (East Eifel, Germany). *Journal of Petrology*, 25, 805–835.
- Wörner, G., Harmon, R.S., Davidson, J., Moorbath, S., Turner, D.L., McMillan, N., Nye, C., Lopez-Escobar, L., and Moreno, H. (1988) The Nevados de Payachata volcanic region (18°S/69°W, N., Chile). I. Geological, geochemical, and isotopic observations. *Bulletin of Volcanology*, 50, 287–303.
- Yoder, H.S.J., and Tilley, C.E. (1962) Origin of basaltic magmas: An experimental study of natural and synthetic rock systems. *Journal of Petrology*, 3, 342–532.